

The Evolution of Energetic Scaling across the Vertebrate Tree of Life

Josef C. Uyeda,^{1,*} Matthew W. Pennell,^{1,2} Eliot T. Miller,¹ Rafael Maia,^{1,3} and Craig R. McClain⁴

1. Department of Biological Sciences and Institute for Bioinformatics and Evolutionary Studies, University of Idaho, Moscow, Idaho 83844;

2. Department of Zoology and Biodiversity Research Centre, University of British Columbia, Vancouver, BC V6T 1Z4, Canada;

3. Department of Ecology, Evolution and Environmental Biology, Columbia University, New York, New York 10027; 4. Department of Biology, Duke University, Durham, North Carolina 27708

Submitted June 7, 2016; Accepted February 3, 2017; Electronically published May 31, 2017

Online enhancements: appendix. Dryad data: <http://dx.doi.org/10.5061/dryad.3c6d2>.

ABSTRACT: Metabolism is the link between ecology and physiology—it dictates the flow of energy through individuals and across trophic levels. Much of the predictive power of metabolic theories of ecology derives from the scaling relationship between organismal size and metabolic rate. There is growing evidence that this scaling relationship is not universal, but we have little knowledge of how it has evolved over macroevolutionary time. Here we develop a novel phylogenetic comparative method to investigate how often and in which clades the macroevolutionary dynamics of the metabolic scaling have changed. We find strong evidence that the metabolic scaling relationship has shifted multiple times across the vertebrate phylogeny. However, shifts are rare and otherwise strongly constrained. Importantly, both the estimated slope and intercept values vary widely across regimes, with slopes that spanned across theoretically predicted values such as 2/3 or 3/4. We further tested whether traits such as ecto-/endothermy, genome size, and quadratic curvature with body mass (i.e., energetic constraints at extreme body sizes) could explain the observed pattern of shifts. Though these factors help explain some of the variation in scaling parameters, much of the remaining variation remains elusive. Our results lay the groundwork for further exploration of the evolutionary and ecological drivers of major transitions in metabolic strategy and for harnessing this information to improve macroecological predictions.

Keywords: metabolic theory of ecology, macroevolution, phylogenetic comparative methods, allometry.

Introduction

Metabolic ecology provides a powerful explanatory link between levels of biological organization from individuals to populations to ecosystems (Van Valen 1976; Felsenstein 1978; Brown et al. 2004; Loreau 2010; Harte 2011; Mc-

Clain et al. 2012). Importantly, much of the predictive power of metabolic ecology derives from rather simple power-law relationships between organismal size and metabolic rate:

$$R = \beta_0 M^{\beta_{\text{mass}}}, \quad (1)$$

where R is the metabolic rate, β_0 is a normalizing constant, M is mass, and β_{mass} is the scaling coefficient. On a logarithmic scale, this becomes a linear relationship:

$$\log(R) = \log(\beta_0) + \beta_{\text{mass}} \log(M). \quad (2)$$

Similar allometric relationships exist between body size and individual growth, individual longevity, population growth rate, and population density (Brown et al. 2004). These relationships suggest the importance of metabolic scaling in determining critical rates of energy flow in individuals that, in turn, scale up to control ecological processes across all levels of organization—from individuals to the biosphere (Brown et al. 2004).

Metabolic allometries provide a powerful connection between metabolic ecology and macroevolution (O'Dwyer et al. 2009; Harte 2011; Yvon-Durocher and Allen 2012; Gilbert et al. 2014; Enquist et al. 2015; Harte et al. 2015). Here we focus specifically on evolutionary allometries, which reflect the long-term effects of adaptation, genetic and developmental constraints, and phylogenetic inertia on species-mean metabolic rates as lineages diverge in body size (Gould 1966; Hansen and Orzack 2005; Pélabon et al. 2014). This is in contrast to ontogenetic allometries and static allometries, which describe the scaling of traits with body size during growth or across individuals of different sizes in a population, respectively. These different types of allometric relationships need not be related (Lande 1979; Chaverud 1982; Pélabon et al. 2014), though the relationship between them is of fundamental evolutionary importance (Muir and Thomas-Huebner 2015). Here we take a macroevolutionary perspective with the goal of finding criti-

* Corresponding author; e-mail: josef.uyeda@gmail.com.

ORCID: Uyeda, <http://orcid.org/0000-0003-4624-9680>; Maia, <http://orcid.org/0000-0002-7563-9795>; McClain, <http://orcid.org/0000-0003-0574-428X>.

Am. Nat. 2017. Vol. 190, pp. 000–000. © 2017 by The University of Chicago. 0003-0147/2017/19002-57034\$15.00. All rights reserved. DOI: 10.1086/692326

cal change points where lineages transitioned to new evolutionary allometric scaling relationships. We refer to these change points as regime shifts, where the regimes themselves may be interpreted as discrete shifts between Simpsonian adaptive zones (Simpson 1944, 1953). Since evolutionary allometries are the by-product of natural selection, drift, and genetic constraints acting over millions of years, such shifts likely reflect changes in the trade-offs constraining divergence. These may result in changes in genetic constraints and/or selective lines of least resistance in the adaptive landscape (Arnold et al. 2001, 2008; Hohenlohe and Arnold 2008).

Changes in the intercept of the allometric scaling relationship, $\log(\beta_0)$, are well documented. However, much discussion has centered on the universality and specific value of the slope, β_{mass} (Glazier 2005, 2010). For metabolic rate, a simple prediction is that β_{mass} equals 2/3, where the ratio of an animal's rate of metabolic heat production and rate of heat dissipation is proportional to the surface-to-volume ratio (Rubner 1883). But as noted decades ago (Kleiber 1932), metabolic rate may scale with body size at slopes greater than 2/3 and instead approximate 3/4 (Brody and Procter 1932). The purported universality of this so-called quarter-power scaling (Savage et al. 2004) in metabolism led to several posited mechanisms to explain its existence (reviewed by Glazier 2010). The most prominent of these is the West-Brown-Enquist (WBE) model, which shows that quarter-power scaling can result if natural selection maximizes efficient transport of nutrients through a fractal network of vessels (West et al. 1997, 1999, 2002), though fractality is not strictly necessary (Banavar et al. 2010). However, the evidence for specific and universal scaling coefficients has been rather mixed and remains contentious (Dodds et al. 2001; White and Seymour 2003; Bokma 2004; Cyr and Walker 2004; Farrell-Gray and Gotelli 2005; Glazier 2005; Sieg et al. 2009; Capellini et al. 2010; McClain et al. 2012; Hudson et al. 2013).

Previous studies have examined the question by dividing lineages into predefined taxonomic units and using them as independent replicates for testing the universality of scaling parameters. However, it is unclear whether the arbitrarily defined taxonomic groupings are likely to capture the true location of shifts in evolutionary allometries. Instead, we seek to discover where shifts in evolutionary allometries occur without a priori expectations or special treatment for named taxonomic groupings. By locating and quantifying the frequency of shifts in the evolutionary allometry, we have a better chance of identifying groups of interest as well as traits or conditions that drive changes in allometric scaling while simultaneously improving macroecological predictions. Furthermore, this approach provides intriguing avenues for asking fundamental questions about the history of ecological systems.

Here we develop a new approach that explicitly models both β_{mass} and β_0 as traits that may evolve on a phylogeny. To investigate the macroevolutionary dynamics of metabolic scaling, we develop a Bayesian method to model the evolution of allometric shifts based on an Ornstein-Uhlenbeck process (Hansen 1997). We use reversible-jump Markov chain Monte Carlo (RJMCMC) machinery (Green 1995) to identify discrete shift points in the evolutionary allometry of metabolism with size (for a related approach, see Uyeda and Harmon 2014). Our method fills a major gap in existing methodology for macroevolutionary studies by providing a tool to discover and model major shifts in the relationships between evolving phenotypic traits. We apply this model to a well-studied data set on metabolic rates and body size from White et al. (2006; hereafter referred to as the White data set). We combined the White data set with phylogenetic data spanning the major vertebrate clades. We then used our model to discover major shifts across the vertebrate tree of life and to test whether shifts in slopes were supported over clade-level shifts in intercept alone.

We emphasize that the approach we present is conceptually and statistically distinct from correcting for phylogeny when estimating the allometric regression, which has been done in a number of previous studies (e.g., Sieg et al. 2009; Capellini et al. 2010; Kolokotronis et al. 2010). The conventional phylogenetic regression model (Grafen 1989) assumes that, while mass and metabolic rate may evolve in a coordinated fashion, the slope itself is assumed to be static. Therefore, these attempts to estimate the slope of the metabolic scaling relationship have assumed (explicitly or implicitly) that the slope is either (i) static across evolutionary time or (ii) changes at the base of a priori-defined major taxonomic groups (Isaac and Carbone 2010) but that it is assumed to be constant within these clades.

A number of factors have been put forth as explanations for the observed variation in both the intercept and the slope, at least in tests that find such variation (Glazier 2005, 2010). Here we focus on three of these predictors: endo-/ectothermy, genome size, and constraints on metabolism at size extremes (i.e., curvature in the evolutionary allometry). First, we account for thermoregulatory strategy in all of our models, as it is known to have wide-ranging importance for an organism's energy budget and we would expect that, all else being equal, endotherms would have higher metabolic demands. Second, genome size has often been linked to metabolic rate either mechanistically (Gregory 2001*b*) or, more commonly, because it is a proxy for cell size, which is thought to be mechanistically linked to metabolic rate (Kozłowski et al. 2003; see "Discussion"). Third, it has been suggested that there is a convex relationship (on a logarithmic scale) between metabolic rate and body size (Zotin et al. 1978; Dodds et al. 2001), especially

in mammals (Kolokotronis et al. 2010). At either extremely small or large sizes, metabolic rates are higher, suggesting fundamental physiological limitations occurring at size extremes (Hanken and Wake 1993). In our analysis, we used model selection to determine whether these factors could explain any of the variation in the allometric scaling parameters.

Methods

Phylogenies

Our analysis spans five major vertebrate clades: mammals, birds, squamate reptiles, amphibians, and bony fish. For birds, squamates, amphibians, and bony fish, we gathered recently published megaphylogenies (Pyron and Wiens 2011; Jetz et al. 2012; Rabosky et al. 2013; Pyron and Burbrink 2014). For the mammals, comprehensive supertrees (Bininda-Emonds et al. 2007) were either in conflict with better resolved trees (e.g., Meredith et al. 2011) or lacked reliable branch lengths, which are necessary for our models. As an alternative, we made use of the collection of phylogenies curated by the Open Tree of Life (OTOL) project (Hinchliff et al. 2015) to construct a synthetic tree based on the best available data—while simultaneously providing a repeatable pipeline for synthesizing growing phylogenetic knowledge within a clade. OTOL contains only cladograms (i.e., the trees do not include branch lengths), and we calibrated the synthetic tree using congruification (Eastman et al. 2013) and previously published time trees found in the OTOL database. Full details on the source trees, calibration points, and bioinformatic pipeline are described in the appendix, available online. We think that merging the OTOL synthetic tree with validated calibrations is likely to be a good option for conducting comparative analyses at large scales, particularly in cases where a reliable species-level tree is unavailable.

We used the Timetree of Life (Hedges et al. 2006) to obtain divergence times between the five major clades and stitch the trees together manually. This allowed us to detect shifts that may have occurred at the base of the major clades. We note that, in practice, the actual divergence times used will have little effect on the analyses if the stem length of each group is large relative to the phylogenetic half-life (Hansen 1997) estimated from the trait models we used.

Trait Data

For our trait data, we combined two previously published collections of metabolic rates and body sizes (McKechnie and Wolf 2004; White et al. 2006). After cleaning the data and temperature correction using the Arrhenius equation (Gillooly et al. 2001), we matched species in the trait data set to the phylogeny (further details on data processing

and temperature correction are provided in the appendix). The final cleaned data sets are deposited in the Dryad data repository: <http://dx.doi.org/10.5061/dryad.3c6d2> (Uyeda et al. 2017).

We obtained genome size data from the animal genome size database (Gregory 2001a) for only 318 of the 857 taxa in our data set. However, given the strong phylogenetic signal in the data, we decided to impute the values for the missing taxa so that we could compare alternative models (see appendix). We fixed the parameters of the Brownian motion process for genome size to their maximum likelihood estimates and drew random values for the unknown tips conditional on the state of the known tips, model parameters, and the phylogeny throughout the course of the Markov chain Monte Carlo (MCMC) analyses. Note that while there are large amounts of missing data, we view our test as conservative since the scenarios under which imputed data will generate spurious relationships are few, and comparisons with smaller data sets with only complete cases suggest that the impact on the qualitative conclusions are minor (see appendix).

We analyzed the data set of Kolokotronis et al. (2010) to try and detect evidence of curvature and resolve conflict with the apparent lack of curvature in the White data set. After matching with our OTOL-generated phylogeny, we obtained a data set that contained 600 taxa. We did not standardize the data set by temperature but instead included a coefficient for the effect of inverse temperature (in Kelvins) in all models in the data set. This was done because the restriction of the data set to mammals simplified analysis of temperature scaling, since all data are assumed to have been measured at approximately the species mean body temperature. Missing body temperatures were imputed using Brownian motion, as was done for genome size.

Analysis

We consider an evolutionary model in which the optimal value of a species trait corresponds to equation (2) but follows an Ornstein-Uhlenbeck (OU) process of evolutionary change on a phylogeny (Hansen 1997). OU models have been widely used in modeling adaptive evolution on phylogenies and correspond to a scenario in which species evolve around a stationary optimum. This OU modeling framework is preferable over other models (e.g., Brownian motion) because the relationship between body mass and metabolic rate is generally explained by constraints and optimality, whereas Brownian motion is unbounded. Here we consider an allometric ridge rather than a single value for the optimum (Hansen et al. 2008). We assume that the predictors in our models are fixed effects and that changes in, for example, mass or genome size have direct, immediate effects on metabolic rate (proportional, of course, to the size of the coefficients for these

variables in the model; Hansen et al. 2008). Shifts in allometric scaling are weighted by previous regimes, so that the metabolic rate of species j ($\ln R_j$) is modeled as

$$\ln R_j = W_{j,\alpha} \boldsymbol{\theta} + \beta_{\text{mass},j} \overline{\ln M_j}, \quad (3)$$

where $W_{j,\alpha}$ is a row vector of weights for each regime θ , $\theta = \ln(\beta_0)$, and $\boldsymbol{\theta}$ is a column vector of all intercept values in the phylogeny. While transitions between adaptive optima are treated as an instantaneous point process, these transitions do not immediately change species trait values as lineages must evolve to reach a new adaptive optimum. Thus, the influence of past adaptive regimes factors into the expected trait values for a species at a given mass. Specifically, the weights in $W_{j,\alpha}$ quantify the influence of time spent in current and past regimes along the path from root to tip—with the weight of past regimes decreasing exponentially proportional to the rate of adaptation, α (for a full description, see Hansen 1997). Here $\beta_{\text{mass},j}$ is the value of β_{mass} in species j 's current regime, with $\overline{\ln M_j}$ indicating the log mass of species j (see a full derivation of eq. [3] in the appendix). When the effects for endothermy, curvature ($\overline{\ln M}$) and genome size ($\overline{\ln \text{GS}}$) are included in the model, these are also treated as fixed effects.

In order to test the hypothesis of evolutionarily dynamic allometric relationships, we need to identify where and when transitions to new evolutionary regimes might have taken place in the phylogeny without any a priori assumptions about the locations of these shifts (i.e., without assuming that major taxonomic groups each had their own optimum; Isaac and Carbone 2010), as well as represent the uncertainty in the placement of these shifts. Reversible-jump Markov chain Monte Carlo (Green 1995) methods are ideally suited for this type of question. In RJMCMC, the dimensionality (number of parameters) of the model is updated during the chain, with new regimes being added (birth proposals) and others combined (death proposals), which has proven fruitful for modeling molecular (Huelssenbeck et al. 2004; Drummond and Suchard 2010) and phenotypic (Eastman et al. 2011; Venditti et al. 2011; Rabosky et al. 2014; Uyeda and Harmon 2014) evolution on phylogenies.

In order to identify locations of statistically supported shifts, we ran a fully reversible-jump model using $\ln R$ as the trait and $\ln M$ and endothermy as predictor variables. We allowed only one shift per branch and set a conditional Poisson prior on the number of shifts with a mean equal to 2.5% the total number of branches in the tree and a maximum number of shifts equal to 5% ($\lambda = 42.85$, $K_{\text{max}} = 86$). Because of the lack of identifiability between endothermy and shifts occurring on the branches leading to birds and mammals, we disallowed shifts in intercept on the branch leading to mammals, so that the coefficient for en-

dothermy represents the shift magnitude in intercept for mammals. Thus, any shift in intercept occurring on the branch leading to birds represents the difference in intercept between mammals and birds. We ran six chains for 1 million generations, sampling every 100 generations, and a burn-in proportion of 0.3. Starting points for each chain were drawn by randomly drawing a number of shifts from the prior distribution and assigning these shifts to branches randomly drawn from the phylogeny with a probability proportional to the size of the clade descended from that branch. We then initialized the MCMC without any birth-death proposals for the first 10,000 generations to improve the fit of the model (otherwise, the models will quickly revert to Brownian motion-like parameters and spend a long period of time before shifts are found). Priors for other parameters were as follows (units follow the semicolon):

$$\alpha \sim \text{half - Cauchy (scale = 1); myr}^{-1}$$

$$\sigma^2 \sim \text{half - Cauchy (scale = 1); } \frac{\ln(\text{mL O}_2 \text{ h}^{-1})^2}{\text{myr}}$$

$$\beta_{\text{mass}} \sim \mathcal{N}(\mu = 0.7, \sigma = 0.1); \frac{\ln(\text{mL O}_2 \text{ h}^{-1})}{\ln(\text{g})}$$

$$\beta_{\text{endo}} \sim \mathcal{N}(\mu = 4.5, \sigma = 0.5); \ln(\text{mL O}_2 \text{ h}^{-1})$$

$$\ln \beta_0 \sim \mathcal{N}(\mu = -2.5, \sigma = 1.75); \ln(\text{mL O}_2 \text{ h}^{-1}).$$

We visualized the analysis by averaging the values of all parameters over each branch and assigning these values to a color ramp (fig. 1).

Our reversible jump failed to converge to a single solution across chains, largely due to different chains fixing on nonidentifiable shift configurations, among which there was poor mixing (but it led to essentially identical inferences). However, overall correlations among branch posterior probabilities were relatively high (median between chains = 0.76, range: 0.70–0.87). For example, sister clades that each have a shift are not identifiable from an ancestral shift in both clades and a subsequent shift in either of the clades. Although our choice of priors can make these alternatives not strictly equivalent, obtaining adequate mixing between stable configurations was found to be nontrivial. Because of these difficulties and the relative complexity of summarizing results across chains, we used our six reversible-jump chains instead to inform the location of shifts and then ran a second set of analyses using only these fixed shift locations. Consequently, we consider the results of this second set of analyses as conditional on the shift locations selected from the summarized reversible-jump analyses.

Fixed shift locations were selected from the six reversible-jump chains by selecting shifts that had an average posterior probability of 0.2 across the post-burn-in samples, which corresponds to an eightfold increase in the posterior probability

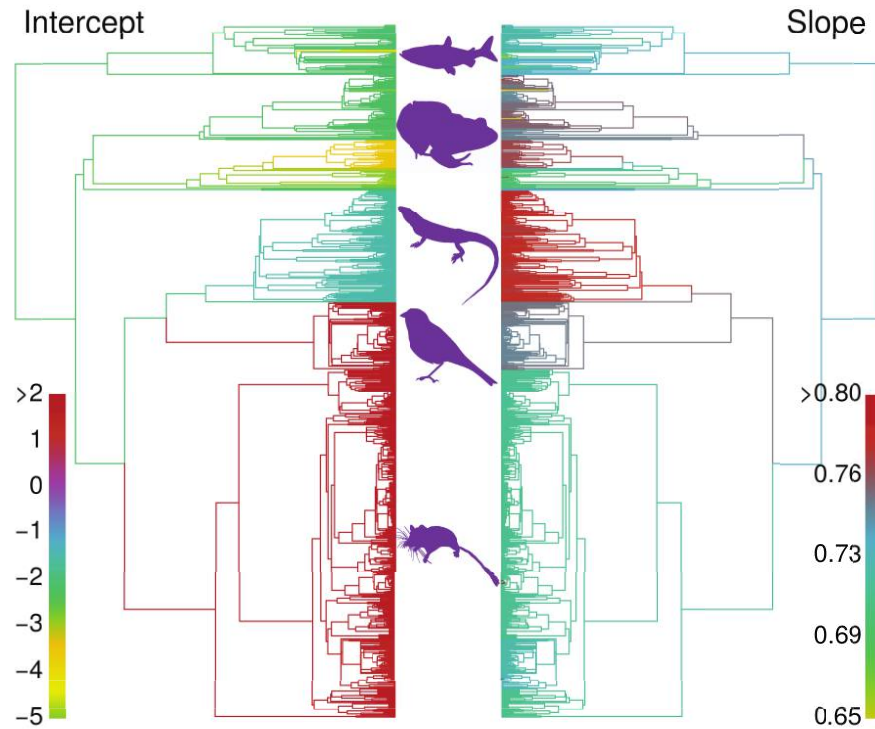


Figure 1: Phylogenetic heat maps of median, branch-specific parameter estimates from reversible-jump analysis of vertebrate metabolic rate data. Both intercept and slope are shown. Data come from the five major clades of vertebrates depicted.

over the prior probability. While somewhat liberal as far as a cutoff, the presence of alternative, nonidentifiable shift configurations has the effect of lowering the posterior probabilities of particular branches. Furthermore, simulation studies have shown that similar approaches have low false-positive rates and that a liberal cutoff is appropriate (Uyeda and Harmon 2014; Khabbazian et al. 2016).

After identifying shifts in the slope and intercept across the phylogeny using RJMCMC, we ran a total of four chains with fixed shifts for 1 million generations, with the first 30% of samples discarded as burn-in. All parameters including optima and slopes had effective sample sizes greater than 150 and appeared to reach convergence across chains (Gelman and Rubin's R statistic for α , σ^2 , root < 1.005). We combined chains to summarize parameter estimates. For all other models, we ran a single chain for 1 million generations and subsequently estimated marginal likelihoods using stepping-stone sampling.

We performed model selection by estimating the marginal likelihood of each model using stepping-stone sampling (Xie et al. 2010) and computing Bayes factors. Each stepping-stone sampler was initialized using the previously run MCMC chain from which a reference function was generated to fit the posterior distribution (Xie et al. 2010). We then ran the stepping-stone sampler across 50 steps drawn from a beta dis-

tribution along the sequence from 0 to 1 with shape parameters of 0.3 and 1, as recommended by Fan et al. (2011).

Once shift locations were chosen from the reversible-jump analysis, we ran a number of models with and without shifts in different parameters. We ran a total of 11 models using fixed shift locations. All models include endothermy, as this transition is well known to cause a major shift in the value of the intercept of the allometric relationship (and, as described above, corresponds to fixing a shift in intercept at the mammal clade, which was supported by the preliminary unconstrained model).

In addition to identifying shifts in the slope and intercept of the allometric relationship across the vertebrate tree of life, we tested whether these shifts were robust to the inclusion of additional predictors that have been previously considered in the field. If some shifts can be explained by the inclusion of these predictors, they likely represent (or are confounded with) the effect of said predictors on the allometric relationship parameters. We demonstrate this by considering models that include a quadratic term relating $\ln R$ to $\ln M^2$, and a coefficient relating $\ln R$ to log genome size ($\ln GS$).

We considered models that included global intercepts and slopes, fixed shifts in intercepts and global slopes, and fixed shifts in intercept and slopes. These three categories

of models were combined in all combinations with either (1) quadratic curvature (β_{mass}^2), (2) genome size (β_{GS}), or (3) genome size and a genome size by mass interaction (β_{GS} and $\beta_{\text{GS} \times \text{mass}}$). For models with genome size coefficients, we also considered models where the shifts in the salamander clades were removed (NS) and shifts where only the Plethodon shift was removed (NP) to test whether shifts in these clades could be explained by the effect of genome size. We ran each model for 1 million generations as a single chain, as described above, discarding the first 30% as burn-in, and checked that each parameter had an effective sample size > 100 using the R package coda.

Finally, we repeated our analysis with the Kolokotronis data set, again starting with a reversible-jump analysis with shifting slopes and intercepts. We used the same priors, including setting the prior on the number of shifts to be 2.5% of the number of nonzero length branches, as in the original analysis. As stated previously, we included a coefficient for the effect of inverse temperature in the model to account for changing body temperatures across mammals. We then repeated the fixed shift analysis as in the White data set, analyzing models with global slopes and intercepts, fixed shifts in intercept and a global slope, and fixed shifts in intercept and slope. These models were combined with and without coefficients for curvature (β_{mass}^2). We also did model selection on the mammals from the White data set. Since few shifts were found in this clade, we considered two models with a global slope and intercept—with and without curvature.

Implementation and Availability

Our approach is implemented in the bayou R package (Uyeda and Harmon 2014). We have made substantial modifications from previous versions of bayou, and an alpha release of bayou is available as a GitHub release (ver. 2.0.0-alpha; <http://dx.doi.org/10.5281/zenodo.47535>; <https://github.com/uyedaj/bayou/tree/dev>). The implementation is designed to be flexible, such that a wide variety of customized regression models can be applied. Scripts to reproduce analyses in this article are available at <https://github.com/uyedaj/bmr>.

Results

Our analyses recovered 29 shifts with posterior probabilities greater than 0.2 (which corresponds to an approximately eightfold increase in posterior probability from the prior). Of these shifts, 17 lead to singleton taxa and 8 shifts lead to clades with five or more taxa. Major shift locations include the stem branches leading to birds, mammals, bats, squamates, snakes, salamanders (two shifts), and the Plethodontidae (lungless salamanders). In a second set of analyses, we fixed the location of these 29 identified shifts to estimate parameters and perform model selection. This was done to facilitate

interpretation of results and ease our computational burden, as exploring more complex models and summarizing posteriors integrated over shift placements can be challenging. In the sections that follow, we therefore report only parameter estimates from these fixed shift analyses (though note that parameter estimates do not differ substantially between fixed and reversible-jump analysis; table A2; tables A1–A3 available online).

In our fixed-shift analyses, we estimated substantial phylogenetic half-life (37.2 myr, 95% highest posterior density [HPD] interval; defined as the narrowest interval that contains 95% of the posterior density: 28.5–46.8). This indicates that even after accounting for clade-level similarity resulting from shifts in allometric regressions, there is substantial phylogenetic signal in the residuals. However, this is still relatively rapid compared to the total tree height of phylogeny (454.6 myr). We also found substantial variability around clade-specific evolutionary allometries, which can be interpreted as the width of the adaptive zone surrounding each allometric line. Specifically, the 95% HPD interval for the stationary distribution of the OU process is estimated to be $\pm 1.15 \log \text{mL O}_2 \text{ h}^{-1}$ wide. In other words, we predict that 95% of the residuals will be within 3.2 times greater or 3.2 times less than the expected metabolic rate (on the raw scale) given the evolutionary allometry of each clade.

Estimates for the slopes across clades showed substantial divergence (fig. 2). Intercepts and slopes for small clades (< 4 species) mostly reflected the prior distributions, as expected. These taxa are outliers, and the data are insufficient to determine whether slope and/or intercept shifts are responsible for the deviations. The root state for the slope (assigned to most fish, frogs, and caecilians) is estimated at 0.78 (95% HPD: 0.73–0.83). For larger clades, we observe slopes ranging from near 0.613 (95% HPD: 0.48–0.74) for non-Plethodontid salamanders to 0.84 (95% HPD: 0.77–0.91) for squamate reptiles. Plethodontid salamanders have a higher slope than the rest of the salamanders (0.796, 95% HPD: 0.66–0.93), while snakes had the same slope as other squamates but a lower intercept. For birds and mammals, the effect of endothermy is estimated to shift the intercept of the allometric regression $4.6 \log \text{mL O}_2 \text{ h}^{-1}$ (95% HPD: 3.9–5.4). Chiropterans were found to have higher slopes (0.814, 95% HPD: 0.72–0.9) than the rest of the mammals (0.700, 95% HPD: 0.67–0.73) but also a lower intercept. In addition, a small clade of Pleuronectinae flatfish were found to have both lower slope and intercept than the root regime but with wide uncertainty associated with these estimates ($\beta_1 = 0.73$, 95% HPD: 0.60–0.85). In addition, all of the other three species of Pleuronectinae flatfish in our data set were singletons assigned their own regimes (also outliers with low metabolic rates relative to their size)—perhaps indicative of increased rates of metabolic rate evolution in this group.

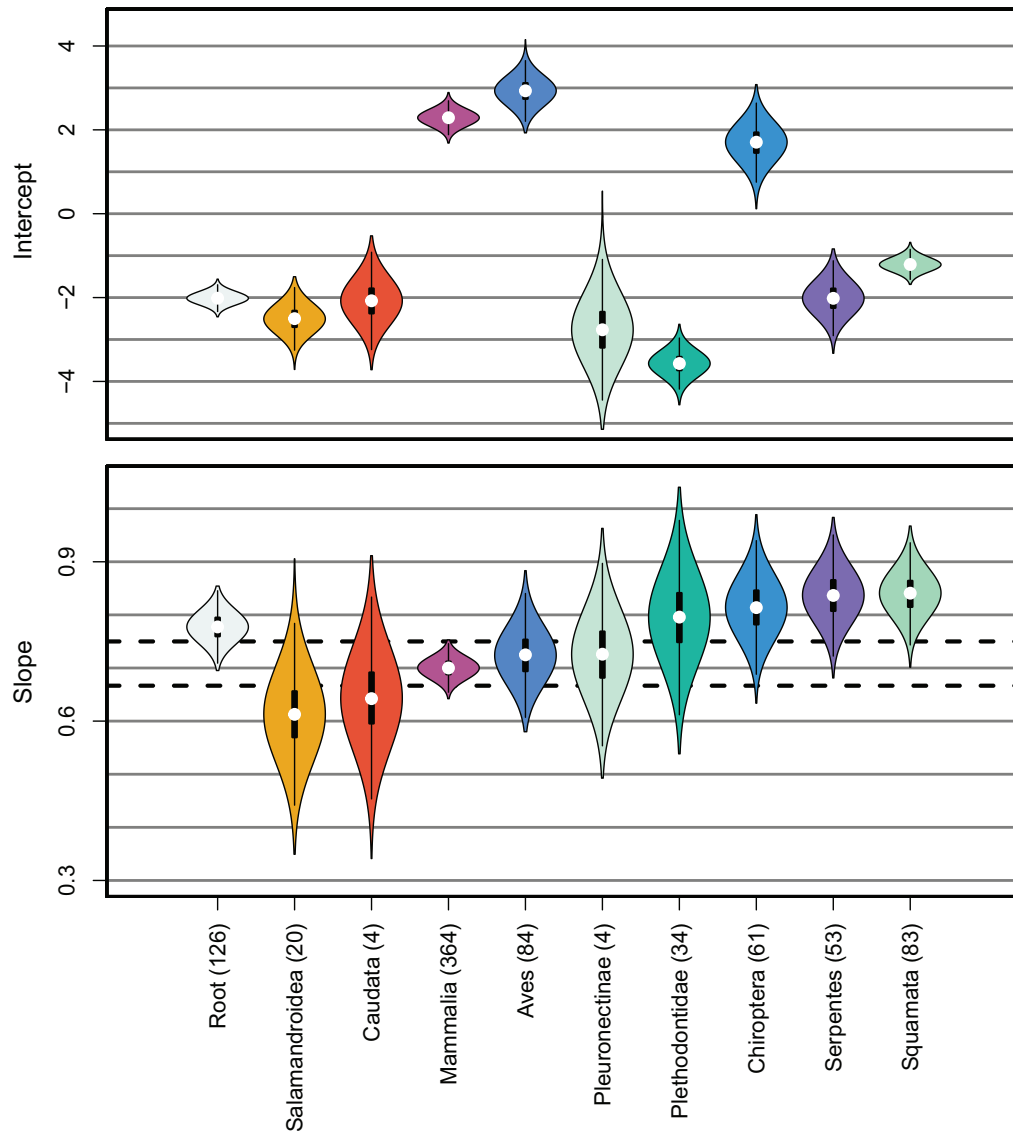


Figure 2: Parameter estimates for major identified clades (using the preliminary reversible-jump Markov chain Monte Carlo analysis) obtained from fixed-shift analyses with separate slopes and intercepts for each shift. Numbers in parentheses indicate the number of species in that group (that do not shift to another state).

We used Bayesian model selection to evaluate the degree of support for shifting intercepts and slopes, as well as additional predictors that may explain the appearance of shifts across the phylogeny. We tested models in which the slope and intercept were either global across the whole tree or were given unique values for each of the 29 identified shifts. A model with separate slopes and intercepts had strong support relative to a model with separate intercepts and a universal slope (table 1; $2 \ln \text{Bayes factor [BF]} = 152.6$). Thus, we have strong evidence for differences in slope across evolutionary groups.

Genome Size

We also tested for the effect of genome size on metabolic rate, with the raw values log transformed and missing data imputed assuming Brownian motion (see appendix). The genome size data set reveals a dramatic shift to larger genome sizes in the salamanders relative to other vertebrates—a group that contained three shifts in our evolutionary allometry analysis (fig. A4; figs. A1–A4 available online). We therefore tested whether shifts in genome size could explain shifts in evolutionary allometry in the salamander

Table 1: Model comparisons for vertebrate phylogeny from the White data set using Bayes factors estimated from stepping-stone sampling

Model	Model code ^a	No. parameters ^b	Marginal ln L	2 ln Bayes factor
$\beta_0 + \beta_{\text{endo}} + \beta_{\text{mass}}$	$0_F M_F$	62	−640.42	0
$\beta_0 + \beta_{\text{endo}} + \beta_{\text{mass}} + \beta_{\text{mass}^2}$	$0_F M_F M^2$	63	−640.89	.93
$\beta_0 + \beta_{\text{endo}} + \beta_{\text{mass}} + \beta_{\text{GS}}$	$0_F M_F G$	65	−641.49	2.12
$\beta_0 + \beta_{\text{endo}} + \beta_{\text{mass}} + \beta_{\text{GS}} + \beta_{\text{GS} \times \text{mass}}$	$0_F M_F G I_{\text{GM}}$	66	−642.59	4.34
$\beta_0 + \beta_{\text{endo}} + \beta_{\text{mass}} + \beta_{\text{mass}^2}$	$0_F M M^2$	34	−716.31	151.76
$\beta_0 + \beta_{\text{endo}} + \beta_{\text{mass}}$	$0_F M$	33	−716.72	152.60
$\beta_0 + \beta_{\text{endo}} + \beta_{\text{mass}} + \beta_{\text{GS}}$	$0_F M G$	35	−717.77	154.69
$\beta_0 + \beta_{\text{endo}} + \beta_{\text{mass}} + \beta_{\text{GS}} + \beta_{\text{GS} \times \text{mass}}$	$0_F M G I_{\text{GM}}$	36	−719.37	157.90
$\beta_0 + \beta_{\text{endo}} + \beta_{\text{mass}}$	$0 M$	5	−750.12	219.40
$\beta_0 + \beta_{\text{endo}} + \beta_{\text{mass}} + \beta_{\text{GS}}$	$0 M G$	6	−750.62	220.40
$\beta_0 + \beta_{\text{endo}} + \beta_{\text{mass}} + \beta_{\text{mass}^2}$	$0 M M^2$	6	−751.18	221.51
$\beta_0 + \beta_{\text{endo}} + \beta_{\text{mass}} + \beta_{\text{GS}} + \beta_{\text{GS} \times \text{mass}}$	$0 M G I_{\text{GM}}$	7	−752.98	225.12
$\beta_0^{-\text{pleth}} + \beta_{\text{endo}} + \beta_{\text{mass}}^{-\text{pleth}} + \beta_{\text{GS}}$	$0_{\text{NP}} M_{\text{NP}} G$	63	−642.86	4.88
$\beta_0^{-\text{sal}} + \beta_{\text{endo}} + \beta_{\text{mass}}^{-\text{sal}} + \beta_{\text{GS}}$	$0_{\text{NS}} M_{\text{NS}} G$	58	−644.26	7.67
$\beta_0^{-\text{pleth}} + \beta_{\text{endo}} + \beta_{\text{mass}}^{-\text{pleth}} + \beta_{\text{GS}} + \beta_{\text{GS} \times \text{mass}}$	$0_{\text{NP}} M_{\text{NP}} G I_{\text{GM}}$	64	−644.37	7.88
$\beta_0^{-\text{sal}} + \beta_{\text{endo}} + \beta_{\text{mass}}^{-\text{sal}} + \beta_{\text{GS}} + \beta_{\text{GS} \times \text{mass}}$	$0_{\text{NS}} M_{\text{NS}} G I_{\text{GM}}$	59	−646.01	11.18

^a Parameters: 0 = β_0 ; M = β_{mass} ; M² = β_{mass^2} ; G = β_{GS} ; I_{GM} = $\beta_{\text{GS} \times \text{mass}}$. Subscripts: none = global; F = fixed shifts found by reversible-jump Markov chain Monte Carlo; NS = fixed shifts but dropping shifts in the salamander (sal) clade; NP = fixed shifts by dropping *Plethodon* (pleth) shift.

^b Number of parameters in the model (including α and σ^2).

clade. Genome size did not improve the fit of the model (BF = 2.12 favoring the simpler model). However, the coefficient for genome size is marginally negative (95% HPD: −0.22, 0.03). Models in which the shifts in the salamander clade were removed given their confounding effect with genome size (which also has at least two major shifts in the salamander clade) also failed to improve on the separate slopes and intercepts model (2 ln BF > 4). However, removal of the salamander shifts tends to increase the magnitude of the negative coefficient for genome size substantially, so that the posterior of the distribution no longer spans zero (fig. 3). For example, in a model where all salamander-specific shifts are removed, the median of the posterior distribution for β_{GS} is −0.20 (95% HPD: −0.30, −0.089; table A2; fig. 3). This corresponds to an approximately 15% decrease in metabolic rate (on the raw scale) for each doubling in genome size. Furthermore, when an interaction between body mass and genome size is included in the model, these coefficients tend to be positive, with the lower 95% CI in different models hovering around zero (table A2; fig. 3). These estimates suggest that increasing genome size likely has the effect of decreasing metabolic rate (intercept) while increasing metabolic rate slopes. However, the complex set of shifts found within the salamander clade cannot be explained by genome size alone.

Curvature

We also tested models including curvature in the relationship in the allometric scaling between body mass and metabolic

rate, as has previously been reported in mammals (Zotin et al. 1978; Dodds et al. 2001; Kolokotronis et al. 2010). Regardless of whether shifts in allometric scaling were included, no models including a quadratic term were more strongly supported than their equivalent nonquadratic models (table 1). Furthermore, quadratic coefficients were all tightly bound around zero, indicating no evidence of universal curvature (fig. A3). When we focused only on the mammalian subset of the White data set, we again found no evidence of universal curvature (table A2; fig. A3). Furthermore, only a single shift was found in the mammalian clade (Chiropterans) besides singletons. These results are in conflict with previously reported findings of Kolokotronis et al. (2010). We further investigated this conflict by repeating the reversible-jump analysis with the same trait data set used by Kolokotronis et al. (2010; hereafter called the Kolokotronis data set, but we note that we used our synthetic mammalian phylogeny for all analyses). We found substantially more shifts in the mammalian clade in the Kolokotronis data set than in the White data set (20 total shifts, nine of which lead to more than one taxon)—many of which were clades not included in the White data set (see appendix for a full list and discussion).

Like with the White data set, models including separate intercepts were preferred over models with global slopes and intercepts using the Kolokotronis data set. However, when curvature was included in this model, the posterior distribution for the quadratic coefficient was always positive and bounded away from 0, indicating a concave curvature to the allometric scaling relationship concordant with previous reported curvature estimates (fig. A3; Kolokotro-

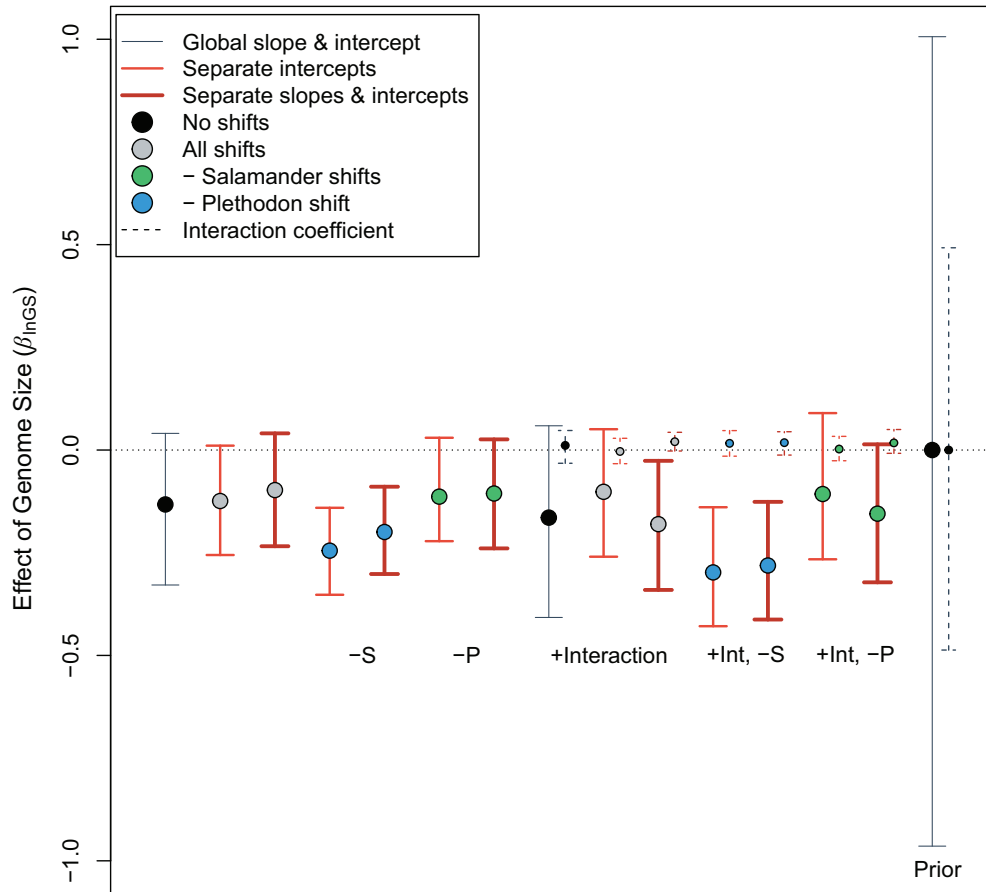


Figure 3: Ninety-five percent highest posterior density estimates for coefficients for the effect of genome size on metabolic rate for various models. The dotted horizontal line indicates no effect ($\beta_{\ln GS} = 0$). Units of the coefficient correspond to the amount of change in log metabolic rate ($\text{mL O}_2 \text{ h}^{-1}$) for an increase of 1 log unit of genome size (C-value).

nes et al. 2010). In fact, Bayesian model selection suggests that a model with only curvature and a global slope and intercept was preferred over a model with shifts (table 2; fig. A3). This suggests that the systematic removal of clades present at the extremes of the body size distribution in the White data set (large marine mammals, ruminants, shrews,

and others) obscured a curvilinear pattern present across mammals evident in the Kolokotronis data set. It appears that shifts in allometric scaling in both slope and intercept in the mammals can be rather simply explained by this curvilinear relationship. Nevertheless, our more general finding is that curvature is not found universally across the

Table 2: Model comparisons for mammals using two different data sets—White et al. (2006) and Kolokotronis et al. (2010)

Data set, model	Model code	No. parameters	Marginal ln L	2 ln Bayes factor
Kolokotronis:				
$\beta_0 + \beta_{\text{mass}} + \beta_{\text{mass}^2} + \beta_{1/\text{temp}}$	0MM ²	6	-177.13	0
$\beta_0 + \beta_{\text{mass}} + \beta_{1/\text{temp}}$	0 _F M	25	-182.50	10.75
$\beta_0 + \beta_{\text{mass}} + \beta_{\text{mass}^2} + \beta_{1/\text{temp}}$	0 _F MM ²	26	-185.55	16.85
$\beta_0 + \beta_{\text{mass}} + \beta_{\text{mass}^2} + \beta_{1/\text{temp}}$	0 _F M _F M ²	46	-192.00	29.75
$\beta_0 + \beta_{\text{mass}} + \beta_{1/\text{temp}}$	0 _F M _F	45	-196.01	37.77
$\beta_0 + \beta_{\text{mass}} + \beta_{1/\text{temp}}$	0M	4	-196.03	37.80
White:				
$\beta_0 + \beta_{\text{mass}}$	0M	5	-189.55	0
$\beta_0 + \beta_{\text{mass}} + \beta_{\text{mass}^2}$	0MM ²	5	-190.51	1.92

vertebrate radiation but is restricted to the mammalian clade.

Discussion

Although the scaling relationship between metabolic rate and body size has been recognized for decades, it has received increased scrutiny following the development of the metabolic theory of ecology (MTE; West et al. 1997, 1999; Brown et al. 2004; see reviews in Glazier 2005, 2010). This simple allometric relationship is often viewed as a lynchpin of the MTE, and therefore finding support for (or rejecting) the hypothesis of $3/4$ scaling has received much scrutiny (Glazier 2010). And while the WBE model is probably the most hotly debated theory of metabolic scaling, it is far from the only one; a wide variety of biophysical models have been put forth to explain $3/4$ scaling, while others have been proposed to explain $2/3$ scaling, and others still for why we should expect variation in this trait (Glazier 2005, 2010). Yet despite the substantial number of empirical tests, disputes remain as to what the pattern of metabolic scaling actually is; different groups, data sets, standardizations, and analytical approaches have provided different answers.

In this article, we propose a shift in perspective: instead of focusing on what the true slope really is, we investigated how this scaling relationship evolved. To be clear, we did not assume a priori that the slope is an evolutionary labile trait: if deviations from a universal scaling slope were due to the idiosyncrasies of species' biology or measurement error (which is probably substantial), then there would be little phylogenetic signal in the data. But this is not what we find when we fit evolutionary models to the data. Rather, we find that throughout the history of vertebrates, there have been a relatively small number of well-supported shifts to new evolutionary regimes with distinct evolutionary optima for both the slope and the intercept relating metabolic rate to body size. We infer that the slope of this evolutionary allometry itself evolves across the vertebrate tree from slightly above $3/4$ to slightly below $2/3$. However, within each evolutionary regime, we observe little change in the allometric parameters over hundreds of millions of years of evolution (see table A3 in the appendix). We do not interpret this as direct evidence for the ubiquity of within-population stabilizing selection on allometric relationships; rather we interpret this as suggesting that within each evolutionary regime, constraints on evolutionary optima generate a narrow ridge of values that species can assume (Hansen 1997; Hansen and Bartoszek 2012; Pennell and Harmon 2013; Uyeda and Harmon 2014). Across the tree, the differences in the intercept are more pronounced; however, within each evolutionary regime, there are still fairly tight constraints (table A3).

While we have characterized the long-term dynamics of the metabolic scaling relationship, the challenge remains to

shifts to specific ecological, physiological, or developmental causes. In other words, what processes and constraints shape the macroevolutionary adaptive landscape (Hansen and Bartoszek 2012) for these traits? Likewise, we do not know to what extent the evolutionary dynamics we describe will alter predictions of community structure and function from macroecological models based on a static metabolic scaling relationship (O'Dwyer et al. 2009; Harte 2011; Yvon-Durocher and Allen 2012; Gilbert et al. 2014; Enquist et al. 2015; Harte et al. 2015). Furthermore, understanding the evolvability of the metabolic scaling relationship will be key to predicting how communities and ecosystems respond to global change (Yvon-Durocher et al. 2010; Dossena et al. 2012; Bruno et al. 2015). We hope our results inspire researchers to incorporate evolving metabolic scaling relationships into existing ecological theory and to evaluate the robustness of ecosystem predictions to variation in the slope and intercept of the relationship (see, e.g., Barneche et al. 2014).

Our results raise a number of important questions, which we admittedly cannot completely answer: What constrains the value of the slope and the intercept both between and within evolutionary regimes (these need not be the same)? When shifts do occur, what types of features—ecological, anatomical, physiological, developmental, or those related to life history—drive these shifts? And, perhaps, most interestingly, what are the downstream consequences and implications for the scaling of metabolism and related metabolic traits?

We find several well-supported shifts in slope. Mammals, salamanders, and squamates have slopes bounded well away from the assumed root state shared by fish and amphibians. Furthermore, within major vertebrate groups, we observe shifts in Plethodontid salamanders and Chiropterans toward higher slopes relative to their ancestors (a result previously observed, but with overlapping confidence intervals; e.g., Kozłowski and Konarzewski 2005; Capellini et al. 2010). Since the reversible-jump analysis we use places equal probability on nearly every branch in the phylogeny, it is notable that shifts are often estimated to correspond to named clades and, further, that many of these groups are known to have interesting life-history characteristics that set them apart from their sister groups. For example, both birds and bats have increased metabolic demands from powered flight (Voigt and Speakman 2007; Shen et al. 2010). Additionally, within the salamanders several unique life-history shifts have occurred that can potentially explain the pattern of shifts in that clade—such as lunglessness and miniaturization in the Plethodontid salamanders and large genome sizes in salamanders as a whole (Hanken and Wake 1993). Other groups—while certainly having unique life histories—do not have obvious candidate explanations and warrant further study (e.g., Pleuronectinae flatfish).

Interestingly, several of these groups we identify have also been found to show evidence of unusual patterns of mitochondrial evolution that may suggest intense selection pressure on metabolic rates. For example, both Plethodontid salamanders and Alethinophidian snakes have both been found to have undergone gene duplications and gene rearrangements in the mitochondrial genome (Mueller and Boore 2005; Castoe et al. 2008), and both Alethinophidian snakes and Chiropterans have evidence of rapid, positive selection in mitochondrial genes responsible for oxidative metabolism that are normally highly conserved across the vertebrates (Castoe et al. 2008; Shen et al. 2010).

Cell size and metabolic rate have been linked empirically (Gregory 2002; Starostová et al. 2009). Genome size has likewise been implicated in the relationship, either as a proxy for cell size (Kozłowski et al. 2003) or perhaps with a direct influence on metabolic rate (Gregory 2001*b*). The reasons why such relationships exist are not well understood. A gradient may exist from small cells that divide frequently, carry little noncoding DNA, and are more metabolically efficient to larger cells that divide infrequently, carry large junk or selfish DNA loads, and are less metabolically efficient (Gregory 2001*b*). Alternatively, cells with larger genomes may require more cellular machinery to function, resulting in decreased metabolic rates (Kozłowski et al. 2003). Despite these theoretical and empirical links, evidence demonstrating the cross-clade relevancy of cell and/or genome size as a mechanism explaining shifts in metabolic rate has been mixed (Licht and Lowcock 1991; Kozłowski et al. 2003; Starostová et al. 2009).

We used our novel approach to test whether shifts in genome size could explain the observed shifts in β_{mass} and θ . Like Kozłowski et al. (2003), we used genome size as a proxy for cell size, though we acknowledge that genome size and cell size are not always closely linked (Pagel and Johnstone 1992). In accord with previous research, we predicted a negative coefficient with genome size, where larger cell sizes decrease metabolism. While we discovered some support for genome size as a mechanism influencing variation in metabolic rate, we found that it does not appear singularly responsible for the observed shifts in scaling. For example, the shift at the base of salamanders could be associated with larger genome sizes, but there are two later shifts within the clade that do not appear related to genome size. This suggests that the dynamics of clade-level shifts within the salamanders are too complex to be explained simply by genome size and may be related to other factors instead of or in combination with the effect of genome size (e.g., lunglessness in Plethodontid salamanders).

Kolokotronis et al. (2010) find a curvature in the scaling of metabolic rates with body size in mammals, positing increases in overall metabolism due to selective constraints at extreme body sizes. Here we find no evidence across

vertebrates for consistent curvature (see also Müller et al. 2012). Furthermore, our initial analysis provided no evidence of curvature in the metabolic scaling within mammals. However, analyzing the Kolokotronis data set, we demonstrate that this apparent discrepancy results from intentional bias in sampling of mammalian taxa in the White data set, in particular by excluding groups that exist at the extremes of the size distribution (e.g., ungulates, aquatic mammals, and shrews).

Furthermore, once we allow for curvature in the Kolokotronis mammalian data set, the clade-specific shifts we identified in mammals are no longer supported. This is an intriguing result. It implies that the evolution of extreme size—across multiple clades of mammals—will be accompanied by nonlinear changes to metabolic rate and that these nonlinear responses are more important than clade-specific differences in ecology or life history. This finding supports the general argument of Kolokotronis et al. (2010) that metabolic constraints may play an important role in the evolution of body sizes, particularly toward the upper tails of the size distribution. However, it remains unclear why this does not appear to be generally true across other vertebrate clades; in these groups, clade-specific shifts are robustly supported (and unlike for the mammals, we have no reason to suspect that very large and very small taxa were systematically excluded from the White data). One simple possibility is that the Kolokotronis data set spanned a much greater range of values for body mass, and mammals contain the taxa with the widest size range in the vertebrates—though it remains clear that the observed shifts in other vertebrate groups cannot be easily explained by curvature. Further exploration of the role of curvature is a ripe topic for future research.

Identifying these factors is of relevance to our understanding of the MTE. In paleobiology, there are long-running debates over whether ecosystem productivity has systematically changed over geological time with the waxing and waning of different lineages (Bambach 1993; Finnegan et al. 2011). While such studies consider the relative abundances and biomasses of different groups, they assume (explicitly or implicitly) that the relationship between mass and metabolic scaling has been fixed throughout history (and specifically that β_{mass} has forever been approximately 3/4). Our finding that this relationship has evolved across vertebrate lineages has profound implications for studying the history of ecosystem bioenergetics.

We would love to be able to draw inferences about the energetic history of vertebrates through time. For instance, has there been a trend toward higher energy efficiency, and what would this imply about food web complexity (Van Valen 1976; Felsenstein 1978; Bambach 1993; Finnegan et al. 2011)? Unfortunately, because we have only metabolic data for contemporary species, we have no ability to detect a historical trend if one were to exist (Slater et al.

2012). Nevertheless, our estimates of the frequency and magnitude of shifts in metabolic scaling could be used to parameterize exploratory simulations or perhaps serve as priors for future analyses involving fossil taxa. Considering the range of possible macroecological outcomes that can result from the range of evolving macroevolutionary parameters may provide important insights into how past ecosystems may have differed from those of today.

Conclusion

Our major finding is twofold: First, throughout the history of vertebrates there have been a small number of significant major evolutionary transitions in the optimal scaling of metabolism in both slope and intercept. Second, for millions and millions of years following these shifts, stasis predominates—the evolution of the metabolic scaling relationship appears to be highly constrained. And, importantly, we find strong evidence against the hypothesis that there is a universal scaling coefficient; natural selection has not pushed each and every vertebrate toward a 2/3 or a 3/4 slope, but instead several major clades and numerous outlier taxa suggest that shifts in life history or changing trade-offs can alter constraints and push taxa along new ridges in phenotypic space. While we cannot explain the placement of all the shifts we have found, our approach provides a foundation for future studies to investigate the ecological, evolutionary, and developmental causes for variation in metabolic scaling. And, more generally, we hope that our findings inspire researchers to work toward synthetic models of biodiversity that leverage information on historical contingency and adaptive potential to refine our predictions of the distribution of organisms through space and time.

Acknowledgments

We would like to specially thank L. Harmon for his encouragement and support. We would also like to thank D. Caetano, D. Collar, and two anonymous reviewers. J.C.U. was funded by National Science Foundation (NSF) award DEB-1208912 to L. Harmon. M.W.P. was supported by Izaak Killam Memorial and Natural Sciences and Engineering Research Council postdoctoral fellowships. E.T.M. was supported by NSF postdoctoral fellowship 1402506. This work was partially supported by a Junior Fellow award from the Simons Foundation to R.M.

Literature Cited

Al-Sadoon, M. K., and N. M. Abdo. 1989. Temperature effects on oxygen consumption of two nocturnal geckos, *Ptyodactylus hasselquistii* (Donndorff) and *Bunopus tuberculatus* Blanford (Reptilia:

- Gekkonidae), in Saudi Arabia. *Journal of Comparative Physiology B* 159:1–4.
- Andrews, R. M., and F. H. Pough. 1985. Metabolism of squamate reptiles: allometric and ecological relationships. *Physiological Zoology* 58:214–231.
- Arnold, S. J., R. Bürger, P. A. Hohenlohe, B. C. Ajie, and A. G. Jones. 2008. Understanding the evolution and stability of the G-matrix. *Evolution* 62:2451–2461.
- Arnold, S. J., M. E. Pfrender, and A. G. Jones. 2001. The adaptive landscape as a conceptual bridge between micro- and macroevolution. *Genetica* 112:9–32.
- Bambach, R. K. 1993. Seafood through time: changes in biomass, energetics, and productivity in the marine ecosystem. *Paleobiology* 19:372–397.
- Banavar, J. R., M. E. Moses, J. H. Brown, J. Damuth, A. Rinaldo, R. M. Sibly, and A. Maritan. 2010. A general basis for quarter-power scaling in animals. *Proceedings of the National Academy of Sciences of the USA* 107:15816–15820.
- Barneche, D., M. Kulbicki, S. Floeter, A. Friedlander, J. Maina, and A. Allen. 2014. Scaling metabolism from individuals to reef-fish communities at broad spatial scales. *Ecology Letters* 17:1067–1076.
- Bininda-Emonds, O. R., M. Cardillo, K. E. Jones, R. D. MacPhee, R. M. Beck, R. Grenyer, S. A. Price, R. A. Vos, J. L. Gittleman, and A. Purvis. 2007. The delayed rise of present-day mammals. *Nature* 446:507–512.
- Bokma, F. 2004. Evidence against universal metabolic allometry. *Functional Ecology* 18:184–187.
- Britton, T., C. L. Anderson, D. Jacquet, S. Lundqvist, and K. Bremer. 2007. Estimating divergence times in large phylogenetic trees. *Systematic Biology* 56:741–752.
- Brody, S., and R. Procter. 1932. Relation between basal metabolism and mature body-weight in different species of mammals and birds. University of Missouri, Agricultural Experimental Station Research Bulletin 166:89–101.
- Brown, J. H., J. F. Gillooly, A. P. Allen, V. M. Savage, and G. B. West. 2004. Toward a metabolic theory of ecology. *Ecology* 85:1771–1789.
- Bruno, J. F., L. A. Carr, and M. I. O'Connor. 2015. Exploring the role of temperature in the ocean through metabolic scaling. *Ecology* 96:3126–3140.
- Capellini, I., C. Venditti, and R. A. Barton. 2010. Phylogeny and metabolic scaling in mammals. *Ecology* 91:2783–2793.
- Castoe, T. A., Z. J. Jiang, W. Gu, Z. O. Wang, and D. D. Pollock. 2008. Adaptive evolution and functional redesign of core metabolic proteins in snakes. *PLoS ONE* 3:e2201.
- Chappell, M. A., and T. M. Ellis. 1987. Resting metabolic rates in boid snakes: allometric relationships and temperature effects. *Journal of Comparative Physiology B* 157:227–235.
- Cheverud, J. M. 1982. Relationships among ontogenetic, static, and evolutionary allometry. *American Journal of Physical Anthropology* 59:139–149.
- Cyr, H., and S. C. Walker. 2004. An illusion of mechanistic understanding. *Ecology* 85:1802–1804.
- Dodds, P. S., D. H. Rothman, and J. S. Weitz. 2001. Re-examination of the “3/4-law” of metabolism. *Journal of Theoretical Biology* 209:9–27.
- Dossena, M., G. Yvon-Durocher, J. Grey, J. M. Montoya, D. M. Perkins, M. Trimmer, and G. Woodward. 2012. Warming alters community size structure and ecosystem functioning. *Proceedings of the Royal Society B* 279, <http://dx.doi.org/10.1098/rspb.2012.0394>.

- Drummond, A. J., and M. A. Suchard. 2010. Bayesian random local clocks, or one rate to rule them all. *BMC Biology* 8:114.
- Eastman, J. M., M. E. Alfaro, P. Joyce, A. L. Hipp, and L. J. Harmon. 2011. A novel comparative method for identifying shifts in the rate of character evolution on trees. *Evolution* 65:3578–3589.
- Eastman, J. M., L. J. Harmon, and D. C. Tank. 2013. Congruification: support for time scaling large phylogenetic trees. *Methods in Ecology and Evolution* 4:688–691.
- Enquist, B. J., J. Norberg, S. P. Bonser, C. Violle, C. T. Webb, A. Henderson, L. L. Sloat, and V. M. Savage. 2015. Scaling from traits to ecosystems: developing a general trait driver theory via integrating trait-based and metabolic scaling theories. *Advances in Ecological Research* 52:249–318.
- Fan, Y., R. Wu, M.-H. Chen, L. Kuo, and P. O. Lewis. 2011. Choosing among partition models in Bayesian phylogenetics. *Molecular Biology and Evolution* 28:523–532.
- Farrell-Gray, C. C., and N. J. Gotelli. 2005. Allometric exponents support a 3/4-power scaling law. *Ecology* 86:2083–2087.
- Felsenstein, J. 1978. Macroevolution in a model ecosystem. *American Naturalist* 112:177–195.
- Finnegan, S., C. M. McClain, M. A. Kosnik, and J. L. Payne. 2011. Escargots through time: an energetic comparison of marine gastropod assemblages before and after the mesozoic marine revolution. *Paleobiology* 37:252–269.
- Gatten, R., K. Miller, and R. Full. 1992. Energetics at rest and during locomotion. Pages 314–377 *in* M. E. Feder and W. W. Burggren, eds. *Environmental physiology of the amphibians*. University of Chicago Press, Chicago.
- Gilbert, B., T. D. Tunney, K. S. McCann, J. P. DeLong, D. A. Vasseur, V. Savage, J. B. Shurin, et al. 2014. A bioenergetic framework for the temperature dependence of trophic interactions. *Ecology Letters* 17:902–914.
- Gillooly, J. F., J. H. Brown, G. B. West, V. M. Savage, and E. L. Charnov. 2001. Effects of size and temperature on metabolic rate. *Science* 293:2248–2251.
- Glazier, D. S. 2005. Beyond the “3/4-power law”: variation in the intra- and interspecific scaling of metabolic rate in animals. *Biological Reviews* 80:611–662.
- . 2010. A unifying explanation for diverse metabolic scaling in animals and plants. *Biological Reviews* 85:111–138.
- Gould, S. J. 1966. Allometry and size in ontogeny and phylogeny. *Biological Reviews* 41:587–638.
- Grafen, A. 1989. The phylogenetic regression. *Philosophical Transactions of the Royal Society B* 326:119–157.
- Green, P. J. 1995. Reversible jump Markov chain Monte Carlo computation and Bayesian model determination. *Biometrika* 82:711–732.
- Gregory, T. R. 2001a. Animal genome size database. <http://www.genomesize.com/>.
- . 2001b. Coincidence, coevolution, or causation? DNA content, cell size, and the C-value enigma. *Biological Reviews* 76:65–101.
- . 2002. A bird’s-eye view of the C-value enigma: genome size, cell size, and metabolic rate in the class Aves. *Evolution* 56:121–130.
- Hanken, J., and D. B. Wake. 1993. Miniaturization of body size: organismal consequences and evolutionary significance. *Annual Review of Ecology and Systematics* 24:501–519.
- Hansen, T. F. 1997. Stabilizing selection and the comparative analysis of adaptation. *Evolution* 51:1341–1351.
- Hansen, T. F., and K. Bartoszek. 2012. Interpreting the evolutionary regression: the interplay between observational and biological errors in phylogenetic comparative studies. *Systematic Biology* 61:413–425.
- Hansen, T. F., and S. H. Orzack. 2005. Assessing current adaptation and phylogenetic inertia as explanations of trait evolution: the need for controlled comparisons. *Evolution* 59:2063–2072.
- Hansen, T. F., J. Pienaar, and S. H. Orzack. 2008. A comparative method for studying adaptation to a randomly evolving environment. *Evolution* 62:1965–1977.
- Harmon, L. J., J. B. Losos, T. J. Davies, R. G. Gillespie, J. L. Gittleman, W. B. Jennings, K. H. Kozak, et al. 2010. Early bursts of body size and shape evolution are rare in comparative data. *Evolution* 64:2385–2396.
- Harte, J. 2011. *Maximum entropy and ecology: a theory of abundance, distribution, and energetics*. Oxford University Press, Oxford.
- Harte, J., A. Rominger, and W. Zhang. 2015. Integrating macroecological metrics and community taxonomic structure. *Ecology Letters* 18:1068–1077.
- Hedges, S. B., J. Dudley, and S. Kumar. 2006. TimeTree: a public knowledge-base of divergence times among organisms. *Bioinformatics* 22:2971–2972.
- Hinchliff, C. E., S. A. Smith, J. F. Allman, J. G. Burleigh, R. Chaudhary, L. M. Coghill, K. A. Crandall, et al. 2015. Synthesis of phylogeny and taxonomy into a comprehensive tree of life. *Proceedings of the National Academy of Sciences of the USA* 112:12764–12769.
- Hohenlohe, P. A., and S. J. Arnold. 2008. MIPoD: a hypothesis-testing framework for microevolutionary inference from patterns of divergence. *American Naturalist* 171:366–385.
- Hudson, L. N., N. J. Isaac, and D. C. Reuman. 2013. The relationship between body mass and field metabolic rate among individual birds and mammals. *Journal of Animal Ecology* 82:1009–1020.
- Huelsenbeck, J. P., B. Larget, and M. E. Alfaro. 2004. Bayesian phylogenetic model selection using reversible jump Markov chain Monte Carlo. *Molecular Biology and Evolution* 21:1123–1133.
- Isaac, N. J., and C. Carbone. 2010. Why are metabolic scaling exponents so controversial? quantifying variance and testing hypotheses. *Ecology Letters* 13:728–735.
- Jetz, W., G. Thomas, J. Joy, K. Hartmann, and A. Mooers. 2012. The global diversity of birds in space and time. *Nature* 491:444–448.
- Khabbazian, M., R. Kriebel, K. Rohe, and C. Ané. 2016. Fast and accurate detection of evolutionary shifts in Ornstein-Uhlenbeck models. *Methods in Ecology and Evolution*, <http://dx.doi.org/10.1111/2041-210X.12534>.
- Kleiber, M. 1932. Body size and metabolism. *Hilgardia* 6:315–353.
- Kolokotronis, T., V. Savage, E. J. Deeds, and W. Fontana. 2010. Curvature in metabolic scaling. *Nature* 464:753–756.
- Kozłowski, J., and M. Konarzewski. 2005. West, Brown and Enquist’s model of allometric scaling again: the same questions remain. *Functional Ecology* 19:739–743.
- Kozłowski, J., M. Konarzewski, and A. Gawelczyk. 2003. Cell size as a link between noncoding DNA and metabolic rate scaling. *Proceedings of the National Academy of Sciences of the USA* 100:14080–14085.
- Lande, R. 1979. Quantitative genetic analysis of multivariate evolution, applied to brain:body size allometry. *Evolution* 33:402–416.
- Licht, L. E., and L. A. Lowcock. 1991. Genome size and metabolic rate in salamanders. *Comparative Biochemistry and Physiology Part B: Comparative Biochemistry* 100:83–92.

- Loreau, M. 2010. From populations to ecosystems: theoretical foundations for a new ecological synthesis. Princeton University Press, Princeton, NJ.
- McClain, C. R., A. P. Allen, D. P. Tittensor, and M. A. Rex. 2012. Energetics of life on the deep seafloor. *Proceedings of the National Academy of Sciences of the USA* 109:15366–15371.
- McKechnie, A. E., and B. O. Wolf. 2004. The allometry of avian basal metabolic rate: good predictions need good data. *Physiological and Biochemical Zoology* 77:502–521.
- Meredith, R. W., J. E. Janečka, J. Gatesy, O. A. Ryder, C. A. Fisher, E. C. Teeling, A. Goodbla, et al. 2011. Impacts of the Cretaceous terrestrial revolution and KPg extinction on mammal diversification. *Science* 334:521–524.
- Mueller, R. L., and J. L. Boore. 2005. Molecular mechanisms of extensive mitochondrial gene rearrangement in plethodontid salamanders. *Molecular Biology and Evolution* 22:2104–2112.
- Muir, C. D., and M. Thomas-Huebner. 2015. Constraint around quarter-power allometric scaling in wild tomatoes (*Solanum* sect. *Lycopersicon*; Solanaceae). *American Naturalist* 186:421–433.
- Müller, D. W., D. Codron, J. Werner, J. Fritz, J. Hummel, E. M. Griebeler, and M. Clauss. 2012. Dichotomy of eutherian reproduction and metabolism. *Oikos* 121:102–115.
- O'Dwyer, J., J. Lake, A. Ostling, V. Savage, and J. Green. 2009. An integrative framework for stochastic, size-structured community assembly. *Proceedings of the National Academy of Sciences of the USA* 106:6170–6175.
- Pagel, M., and R. A. Johnstone. 1992. Variation across species in the size of the nuclear genome supports the junk-DNA explanation for the C-value paradox. *Proceedings of the Royal Society B* 249:119–124.
- Pélabon, C., C. Firmat, G. H. Bolstad, K. L. Voje, D. Houle, J. Cassara, A. L. Rouzic, and T. F. Hansen. 2014. Evolution of morphological allometry. *Annals of the New York Academy of Sciences* 1320:58–75.
- Pennell, M. W., J. M. Eastman, G. J. Slater, J. W. Brown, J. C. Uyeda, R. G. FitzJohn, M. E. Alfaro, and L. J. Harmon. 2014. geiger v2.0: an expanded suite of methods for fitting macroevolutionary models to phylogenetic trees. *Bioinformatics* 30:2216–2218.
- Pennell, M. W., and L. J. Harmon. 2013. An integrative view of phylogenetic comparative methods: connections to population genetics, community ecology, and paleobiology. *Annals of the New York Academy of Sciences* 1289:90–105.
- Pyron, R. A., and F. T. Burbrink. 2014. Early origin of viviparity and multiple reversions to oviparity in squamate reptiles. *Ecology Letters* 17:13–21.
- Pyron, R. A., and J. J. Wiens. 2011. A large-scale phylogeny of amphibia including over 2800 species, and a revised classification of extant frogs, salamanders, and caecilians. *Molecular Phylogenetics and Evolution* 61:543–583.
- Rabosky, D. L., S. C. Donnellan, M. Grundler, and I. J. Lovette. 2014. Analysis and visualization of complex macroevolutionary dynamics: an example from Australian scincid lizards. *Systematic Biology* 63:610–627.
- Rabosky, D. L., F. Santini, J. Eastman, S. A. Smith, B. Sidlauskas, J. Chang, and M. E. Alfaro. 2013. Rates of speciation and morphological evolution are correlated across the largest vertebrate radiation. *Nature Communications* 4:1958.
- Ruben, J. A. 1976. Aerobic and anaerobic metabolism during activity in snakes. *Journal of Comparative Physiology* 109:147–157.
- Rubner, M. 1883. Ueber den einfluss der korpergrösse auf stoffund kraftwechsel. *Zeitschrift für Biologie* 19:535–562.
- Savage, V. M., J. Gillooly, W. Woodruff, G. West, A. Allen, B. Enquist, and J. Brown. 2004. The predominance of quarter-power scaling in biology. *Functional Ecology* 18:257–282.
- Shen, Y.-Y., L. Liang, Z.-H. Zhu, W.-P. Zhou, D. M. Irwin, and Y.-P. Zhang. 2010. Adaptive evolution of energy metabolism genes and the origin of flight in bats. *Proceedings of the National Academy of Sciences of the USA* 107:8666–8671.
- Sieg, A. E., M. P. O'Connor, J. N. McNair, B. W. Grant, S. J. Agosta, and A. E. Dunham. 2009. Mammalian metabolic allometry: do intraspecific variation, phylogeny, and regression models matter? *American Naturalist* 174:720–733.
- Simpson, G. G. 1953. The major features of evolution. Columbia University Press, New York.
- . 1944. Tempo and mode in evolution. Columbia University Press, New York.
- Slater, G. J., L. J. Harmon, and M. E. Alfaro. 2012. Integrating fossils with molecular phylogenies improves inference of trait evolution. *Evolution* 66:3931–3944.
- Starostová, Z., L. Kubička, M. Konarzewski, J. Kozłowski, and L. Kratochvíl. 2009. Cell size but not genome size affects scaling of metabolic rate in eyelid geckos. *American Naturalist* 174:E100–E105.
- Tsuji, J. S. 1988. Thermal acclimation of metabolism in *Sceloporus* lizards from different latitudes. *Physiological Zoology* 3:241–253.
- Uyeda, J. C., and L. J. Harmon. 2014. A novel Bayesian method for inferring and interpreting the dynamics of adaptive landscapes from phylogenetic comparative data. *Systematic Biology* 63:902–918.
- Uyeda, J. C., M. W. Pennell, E. T. Miller, R. Maia, and C. R. McClain. 2017. Data from: The evolution of energetic scaling across the vertebrate tree of life. Dryad Digital Repository, <http://dx.doi.org/10.5061/dryad.3c6d2>.
- Van Valen, L. 1976. Energy and evolution. *Evolutionary Theory* 1:179–229.
- Venditti, C., A. Meade, and M. Pagel. 2011. Multiple routes to mammalian diversity. *Nature* 479:393–396.
- Voigt, C., and J. Speakman. 2007. Nectar-feeding bats fuel their high metabolism directly with exogenous carbohydrates. *Functional Ecology* 21:913–921.
- West, G. B., J. H. Brown, and B. J. Enquist. 1997. A general model for the origin of allometric scaling laws in biology. *Science* 276:122–126.
- . 1999. The fourth dimension of life: fractal geometry and allometric scaling of organisms. *Science* 284:1677–1679.
- West, G. B., W. H. Woodruff, and J. H. Brown. 2002. Allometric scaling of metabolic rate from molecules and mitochondria to cells and mammals. *Proceedings of the National Academy of Sciences of the USA* 99:2473–2478.
- White, C. R., N. F. Phillips, and R. S. Seymour. 2006. The scaling and temperature dependence of vertebrate metabolism. *Biology Letters* 2:125–127.
- White, C. R., and R. S. Seymour. 2003. Mammalian basal metabolic rate is proportional to body mass $2/3$. *Proceedings of the National Academy of Sciences of the USA* 100:4046–4049.
- Wood, S. C., K. Johansen, M. L. Glass, and G. Maloiy. 1978. Aerobic metabolism of the lizard *Varanus exanthematicus*: effects of activity, temperature, and size. *Journal of Comparative Physiology* 127:331–336.
- Xie, W., P. O. Lewis, Y. Fan, L. Kuo, and M.-H. Chen. 2010. Improving marginal likelihood estimation for Bayesian phylogenetic model selection. *Systematic Biology* 60:150–160.

Yvon-Durocher, G., and A. P. Allen. 2012. Linking community size structure and ecosystem functioning using metabolic theory. *Philosophical Transactions of the Royal Society B* 367:2998–3007.

Yvon-Durocher, G., J. I. Jones, M. Trimmer, G. Woodward, and J. M. Montoya. 2010. Warming alters the metabolic balance of ecosystems. *Philosophical Transactions of the Royal Society B* 365:2117–2126.

Zotin, A., V. Konoplev, and V. Grudnitsky. 1978. The questions of non-linearity for using criterion of orderliness. Pages 361–370 in I. Lamprecht and A. I. Zotin, eds. *Thermodynamics of biological processes*. W. de Gruyter, Berlin.

Associate Editor: David C. Collar
Editor: Alice A. Winn



A plethodontid salamander (*Desmognathus ocoee*) from North Carolina. Photo credit: Josef C. Uyeda.